

# Uncertain Darcy's problem and the stochastic particle transport

Giacomo Garegnani

Supervisors: Dr. Sebastian Krumscheid and Prof. Fabio Nobile

## Contents

<b>1</b>	<b>Expected exit time from a domain</b>	<b>2</b>
1.1	Numerical Methods . . . . .	2
1.1.1	Discrete Euler-Maruyama . . . . .	2
1.1.2	Continuous Euler-Maruyama. . . . .	3
1.1.3	Reflecting boundaries . . . . .	4
1.2	A PDE approach . . . . .	4
1.3	One-Dimensional Case . . . . .	5
1.3.1	Analytical expression of the mean exit time . . . . .	6
1.3.2	Numerical experiments - Estimation of $\tau$ . . . . .	6
1.3.3	Numerical approximation of $\Phi$ with the PDE approach . . . . .	8
1.3.4	Numerical experiments - Estimation of $\Phi$ . . . . .	9
1.4	Two-dimensional case . . . . .	9
1.4.1	Numerical experiments - Estimation of $\tau$ . . . . .	9
1.4.2	Numerical experiments - Estimation of $\Phi$ . . . . .	10
<b>2</b>	<b>The uncertain Darcy problem</b>	<b>12</b>
2.1	Problem statement . . . . .	12
2.2	Finite Elements solution of the Darcy problem . . . . .	13
2.3	Solution of the SDE . . . . .	14

# 1 Expected exit time from a domain

We aim to estimate the exit time of a particle driven by a deterministic transport field and a stochastic diffusion from a domain  $D \subset \mathbb{R}^d$ . Given a vector  $W(t)$  of  $m$  independent Brownian motions and two functions  $f: \mathbb{R}^d \rightarrow \mathbb{R}^d, g: \mathbb{R}^d \rightarrow \mathbb{R}^{d \times m}$ , we consider the following stochastic differential equation (SDE)

$$\begin{cases} dX(t) = f(X(t))dt + g(X(t))dW(t), & 0 < t \leq T, \\ X(0) = X_0, & X_0 \in D. \end{cases} \quad (1)$$

The problem is completed with two different types of boundary conditions, namely

- i. *killing boundaries*: if the particle exits  $D$  the process is stopped,
- ii. *reflecting boundaries*: the particle trajectory is reflected normally inside  $D$  when it touches the boundary  $\partial D$ .

Our aim is to estimate numerically the first exit time of the solution  $X(t)$  from  $D$ , *i.e.*, the quantity

$$\tau = \min\{\min\{t: X(t) \notin D\}, T\}. \quad (2)$$

Let us remark that the parameter  $\tau$  is meaningful only if there exists a portion of the boundary  $\Gamma_k \subset \partial D$  that is endowed with killing boundary conditions. Otherwise, the process  $X(t)$  will stay in  $D$  for the whole time interval, giving as a result  $\tau = T$  for each realisation of  $X(t)$ . Another quantity of interest is defined as follows

$$\phi = \phi(T, X_0, F) = \mathbb{1}_{\{\tau < T\}} F(X(T)), \quad (3)$$

where  $F: \mathbb{R}^d \rightarrow \mathbb{R}$  is a smooth function. An interesting choice of  $F$  could be the function mapping every  $x$  of  $\mathbb{R}^d$  to the value 1. In this case, the expectation of  $\phi$  is equal to the probability for  $X(t)$  to exit the domain before the final time  $T$ . Let us choose the notation  $F = 1$  in this case, getting

$$\Phi(T, X_0) = \mathbb{E}(\phi(T, X_0, 1)) = \Pr(\tau < T | X(0) = X_0) \quad (4)$$

In the case of general  $f, g$  and for a  $d$ -dimensional SDE, there is no closed form for  $\tau$  and  $\phi$ . Therefore, we approximate the value of  $\tau$  by means of two numerical schemes, briefly presented in the following.

## 1.1 Numerical Methods

### 1.1.1 Discrete Euler-Maruyama

Given  $N \in \mathbb{N}$  let us define a partition of  $[0, T]$  as  $P_h = \{t_i\}_{i=0}^N, t_i = ih, h = T/N$ . The Discrete Euler-Maruyama method (DEM) for problem (1) is defined as follows

$$\begin{cases} X_h^d(t_{i+1}) = f(X_h^d(t_i))h + g(X_h^d(t_i))(W(t_{i+1}) - W(t_i)), \\ X_h^d(0) = X_0. \end{cases} \quad (5)$$

The exit time  $\tau$  is approximated with the quantity  $\tau_h^d$  defined as

$$\tau_h^d = \min\{\min\{t_i: X_h^d(t_i) \notin D\}, T\}. \quad (6)$$

We approximate analogously  $\phi$  as

$$\phi_h^d = \mathbb{1}_{\{\tau_h^d < T\}} F(X_h^d(T)). \quad (7)$$

Let us state two results concerning the weak error of this method.

**Proposition 1.1** *Under appropriate assumptions of smoothness of  $f, g, D, \partial D, F$ ,*

$$|\mathbb{E}(\tau_h^d) - \mathbb{E}(\tau)| = O(\sqrt{h}). \quad (8)$$

**Proposition 1.2** *Under appropriate assumptions of smoothness of  $f, g, D, \partial D, F$ ,*

$$|\mathbb{E}(\phi_h^d) - \mathbb{E}(\phi)| = O(\sqrt{h}). \quad (9)$$

An discussion of result 1.1 can be found in [5], its proof in [3]. A proof of 1.2 can be found in [1].

### 1.1.2 Continuous Euler-Maruyama.

Let us consider the partition  $P_h$  of  $[0, T]$  as above. The Continuous Euler-Maruyama (CEM) method is defined as

$$\begin{cases} X_h^c(t) = f(X(t_i))(t - t_i) + g(X(t_i))(W(t) - W(t_i)), & t_i < t \leq t_{i+1}, \\ X_h^c(0) = X_0. \end{cases} \quad (10)$$

Let us remark that in case the particle does not exit the domain,  $X_h^c(t_i) = X_h^d(t_i)$  for all  $t_i \in P_h$ . It is possible to compute the probability that a particle has exited the domain at a time  $t$  between two consecutive timesteps  $t_i, t_{i+1}$  when  $D$  is an half-space with the following formula [2]

$$\mathbb{P}(\exists t \in [t_i, t_{i+1}] \quad X_h^d(t) \notin D | X_h^d(t_i) = x_i, X_h^d(t_{i+1}) = x_{i+1}) = p(x_i, x_{i+1}, h), \quad (11)$$

with  $p(x_i, x_{i+1}, h)$  given by

$$p(x_i, x_{i+1}, h) = \exp \left( -2 \frac{[n \cdot (x_i - z_i)][n \cdot (x_{i+1} - z_i)]}{hn \cdot (gg^T(x_i)n)} \right), \quad (12)$$

where  $z_i$  is the projection of  $x_i$  on  $\partial D$  and  $n$  is the normal to  $\partial D$  in  $z_i$ . At each timestep  $t_{i+1}$  we compute the probability  $p(x_i, x_{i+1}, h)$ , and then simulate a variable  $U$  distributed uniformly in the interval  $[0, 1]$ , thus obtaining a realization  $u$ . Hence, we conclude that the particle has left the domain for a time  $t$  in  $(t_i, t_{i+1})$  if  $u$  is smaller than  $p$ . Therefore, we approximate the exit time as

$$\tau_h^c = \min\{T, \min\{t_i = hi : X_h(t_i) \notin D\}, \min\{t_i = hi : u < p(x_{i-1}, x_i, h)\}\}, \quad (13)$$

In the same way as in DEM, we can approximate  $\phi$  as

$$\phi_h^c = \mathbb{1}_{\{\tau_h^c < T\}} F(X_h^c(T)). \quad (14)$$

We show the pseudocode for the implementation of CEM in Algorithm 1.

The weak error of this method has been studied exhaustively in previous work.

**Proposition 1.3** *Under appropriate smoothness assumptions,*

$$|\mathbb{E}(\phi_h^c) - \mathbb{E}(\phi)| = O(h). \quad (15)$$

A proof of result 1.3 can be found in [2].

**Algorithm 1:** Continuous Euler-Maruyama

```

for  $t_i \in P_h$  do
   $X(t_{i+1}) = f(X(t_i))h + g(X(t_i))(W(t_{i+1}) - W(t_i))$  ;
  if  $X(t_{i+1}) \notin D$  then
     $\tau_h^c = t_{i+1}$  ;
     $\phi_h^c = F(X_h^c(t_{i+1}))$  ;
    return;
  else
    compute  $p = p(x_i, x_{i+1}, h)$  ;
    simulate  $u \sim \text{Unif}(0, 1)$  ;
    if  $u < p$  then
       $\tau_h^c = t_{i+1}$  ;
       $\phi_h^c = F(X_h^c(t_{i+1}))$  ;
      return;
    end
  end
end

```

**1.1.3 Reflecting boundaries**

The reflecting boundaries are treated in the same way for both DEM and CEM. Let us denote by  $\Gamma_k$  and  $\Gamma_r$  the killing and reflecting subsets of  $\partial D$ , *i.e.*

$$\Gamma_r \cup \Gamma_k = \partial D, \quad \Gamma_r \cap \Gamma_k = \emptyset \quad (16)$$

In case the particle approaches  $\Gamma_k$  the exit is treated as above. If for a timestep of  $t_i \in P_h$ ,  $X(t_i)$  is not in  $D$  and has crossed  $\Gamma_r$  at a time  $t_{i-1} < t < t_i$ , we update the solution to be the normal reflection inside  $D$  of  $X(t_i)$ .

**1.2 A PDE approach**

It is possible to express the mean exit time and the probability of exit from a domain in terms of the solution of partial differential equations (PDE's). Let us denote by  $\Gamma_k, \Gamma_r$  the killing and reflecting subsets of  $\partial D$ . We consider then the expectation of the exit time from the domain  $D$  for a trajectory that at  $t = 0$  is at position  $x$ , *i.e.*,

$$\bar{\tau}(x) = \mathbb{E}(\tau | X(0) = x). \quad (17)$$

Let us define the operator  $\mathcal{L}$  induced by (1) acts on a function  $u: \mathbb{R}^d \rightarrow \mathbb{R}$  as follows

$$\mathcal{L}u = f \cdot \nabla u + \frac{1}{2} g g^T : \nabla \nabla u, \quad (18)$$

where the  $:$  operator between two matrices  $A, B$  in  $\mathbb{R}^{d \times d}$  is defined as follows

$$A : B = \sum_{i,j=1}^d \{A\}_{ij} \{B\}_{ij} = \text{tr}(A^T B). \quad (19)$$

The following result allows computing the mean exit time as the solution of an appropriate PDE.

**Proposition 1.4** *Let  $\mathcal{L}$  be the differential operator defined as (18). Then, if  $\Gamma_k$  and  $\Gamma_r$  are respectively the killing and reflecting subsets of  $\partial D$ , such that  $\Gamma_k \cup \Gamma_r = \partial D$ ,  $\Gamma_k \cap \Gamma_r = \emptyset$ , the mean exit time  $\bar{\tau}(x)$  for the solution  $X(t)$  of (1) with  $X_0 = x$  is the solution of the following boundary value problem*

$$\begin{cases} \mathcal{L}\bar{\tau}(x) = -1, & \text{in } D, \\ \bar{\tau}(x) = 0, & \text{on } \Gamma_k, \\ \nabla \bar{\tau}(x) \cdot n = 0, & \text{on } \Gamma_r, \end{cases} \quad (20)$$

where  $n$  is the normal to  $\Gamma_r$ .

Further analytical treatment of the mean exit time can be found in [6, 8].

We now consider the probability of exit from  $D$  for a solution  $X(t)$  that is equal to  $x$  for  $t = s < T$ . This probability is the solution of a boundary value problem.

**Proposition 1.5** *Let  $\mathcal{L}$  be the differential operator defined as (18). Then, if  $\Gamma_k$  and  $\Gamma_r$  are respectively the killing and reflecting subsets of  $\partial D$ , such that  $\Gamma_k \cup \Gamma_r = \partial D$ ,  $\Gamma_k \cap \Gamma_r = \emptyset$*

$$\Pr(\tau < T | X(s) = x) = \Phi(x, s, T) \quad (21)$$

where  $\Phi(x, t, T)$  is the solution of the following backwards PDE

$$\begin{cases} \frac{\partial}{\partial t} \Phi(x, t, T) + \mathcal{L}\Phi(x, t, T) = 0 & \text{in } D, s \leq t < T, \\ \Phi(x, t, T) = 1 & \text{on } \Gamma_k, s \leq t \leq T, \\ \nabla \Phi(x, t, T) \cdot n = 0, & \text{on } \Gamma_r, s \leq t \leq T, \\ \Phi(x, T, T) = 0 & \text{in } D, \end{cases} \quad (22)$$

where  $n$  is the normal to  $\Gamma_r$ .

The proof in case  $\Gamma_k = \partial D$  of this result can be found in [9]. Further treatment in case of mixed boundary conditions and the closed form of the solution for some particular geometries of  $D \subset \mathbb{R}^2$  can be found in [4]. It is therefore possible to approximate  $\bar{\tau}$  and  $\Phi$  by means of classical methods for solving PDE's numerically, such as finite differences or the Finite Elements Method.

### 1.3 One-Dimensional Case

We consider problem (1) in case  $d = 1$ . Given  $f, g: \mathbb{R} \rightarrow \mathbb{R}$ , an interval  $D = [l, r]$  and a Brownian motion  $W(t)$ , let us consider the following one dimensional SDE

$$\begin{cases} dX(t) = f(X(t))dt + g(X(t))dW(t), & 0 < t \leq T, \\ X(0) = X_0, & X_0 \in D. \end{cases} \quad (23)$$

In this case, the boundary of  $D$  consists of the two points  $\{l, r\}$ . In order for the problem of the determination of  $\tau$  to be meaningful, at least one of the two points should be endowed with a killing boundary condition.

### 1.3.1 Analytical expression of the mean exit time

In this simple frame, it is possible to deduce an analytical solution  $\bar{\tau}$  of (20). Let us consider the boundary condition at  $x = l$  fixed as *killing* and vary the boundary condition at  $x = r$ . Since the scope is deducing the exit time of a particle from  $D$ , this assumption is plausible. In this frame, it is possible to rewrite (20) as

$$\left\{ \begin{array}{l} f(x)\bar{\tau}'(x) + \frac{1}{2}g^2(x)\bar{\tau}''(x) = -1, \quad l < x < r, \\ \bar{\tau}(l) = 0, \\ \bar{\tau}(r) = 0, \quad \text{if for } x = r \text{ the boundary is } \textit{killing}, \\ \bar{\tau}'(r) = 0, \quad \text{if for } x = r \text{ the boundary is } \textit{reflecting}. \end{array} \right. \quad (24)$$

It is possible to show [6, 8] that  $\bar{\tau}$  is in the one-dimensional case given by

$$\bar{\tau}(x) = -2 \int_l^x \exp(-\psi(z)) \int_l^z \frac{\exp(\psi(y))}{g^2(y)} dy + c_1 \int_l^x \exp(-\psi(y)) dy + c_2, \quad (25)$$

where the function  $\psi$  is defined as

$$\psi(x) = \int_l^x \frac{2f(y)}{g^2(y)} dy, \quad (26)$$

and the constants  $c_1, c_2 \in \mathbb{R}$  depend on the boundary conditions as follows

$$\begin{aligned} c_1 &= 2 \frac{\int_l^r \exp(-\psi(z)) \int_l^z \frac{\exp(\psi(y))}{g^2(y)} dy}{\int_l^r \exp(-\psi(y)) dy}, \quad \text{if for } x = r \text{ the boundary is } \textit{killing}, \\ c_1 &= 2 \int_l^r \frac{\exp(-\psi(y))}{g(y)^2} dy, \quad \text{if for } x = r \text{ the boundary is } \textit{reflecting}, \\ c_2 &= 0. \end{aligned} \quad (27)$$

Let us remark that in case  $f = -V'$  for some smooth function  $V$  and  $g = \sigma \in \mathbb{R}$ , the expression of  $\psi$  simplifies to

$$\psi(x) = 2 \frac{V(l) - V(x)}{\sigma^2}. \quad (28)$$

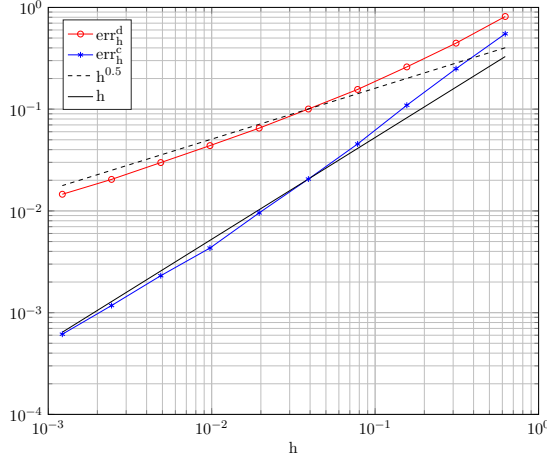
The value for the expected exit time given by (25) will be used as a reference for verifying the order of convergence of the numerical methods.

### 1.3.2 Numerical experiments - Estimation of $\tau$

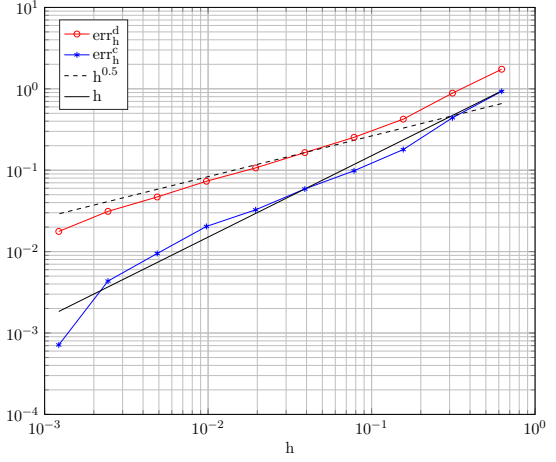
**Smooth case.** We consider as a domain for (23) the interval  $D = [-1, 1]$ , final time  $T = 5$  and the following functions

$$\begin{aligned} f(x) &= -V'(x), \quad \text{where } V(x) = 0.1(8x^4 - 8x^2 + x + 2), \\ g(x) &= \sigma = 3. \end{aligned} \quad (29)$$

We approximate the value of  $\tau$  with a Montecarlo simulation of  $\tau_h^d$  and  $\tau_h^c$  computed as in (6) and (13) from the solutions provided by DEM and CEM respectively. In order to verify the order of convergence of the methods, we let  $N$  vary in the set  $2^i, i = 3, \dots, 12$  and we fix the number of trajectories  $M$  to 10000. In this way, the error caused by the Montecarlo estimation should not spoil the order of convergence. In Figure 1 we show the errors obtained fixing  $X_0 = 0$  in both the cases of killing and reflecting boundary

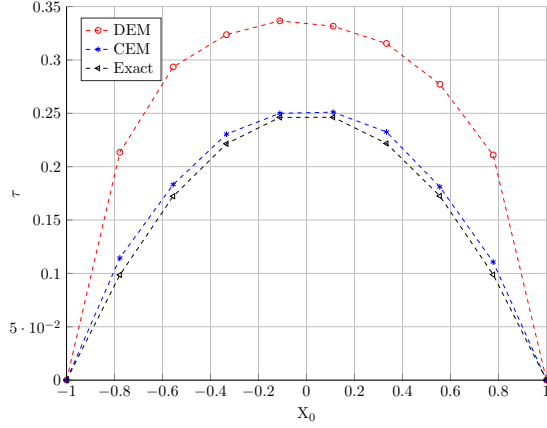


(a) Killing boundary in  $x = 1$

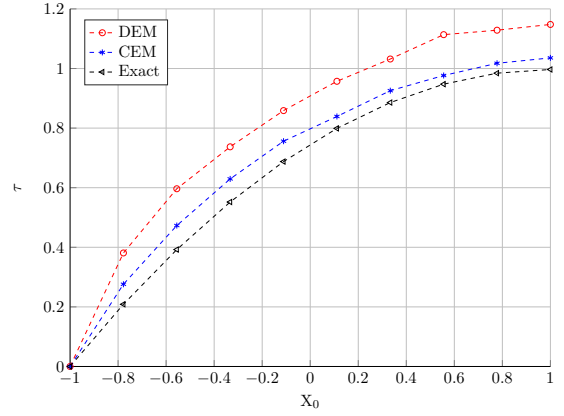


(b) Reflecting boundary in  $x = 1$

Figure 1: Orders of convergence for DEM and CEM in the one-dimensional case.



(a) Killing boundary in  $x = 1$



(b) Reflecting boundary in  $x = 1$

Figure 2: Approximation of  $\tau$  for the discrete and continuous EM method in the one-dimensional case.

conditions in  $x = 1$ . Moreover, in Figure 2 we show an approximation of  $\tau$  obtained with the two methods with  $h = T/128$  and  $M = 1000$  for a set of 10 initial values equispaced along  $D$ . It is possible to remark that computing the probability of exit between two consecutive timesteps as in (12) allows correcting the overestimation of  $\tau$  obtained simply using DEM. We want to estimate the computational time for both the method. We consider  $M = 10000$ , killing boundary conditions and  $N = 2^i, i = 3, \dots, 12$ . It is possible to remark in Figure 3 that the computational time required by CEM is higher than for DEM if the same value of  $h$  is employed. On the other hand, fixing the error, CEM is faster than DEM in this case.

**Rough case.** We consider the same domain  $D$  as above,  $T = 5$  and  $g = \sigma = 3$ . We consider  $V$  to be piecewise linear, so that  $f = -dV$  is piecewise constant. In particular,

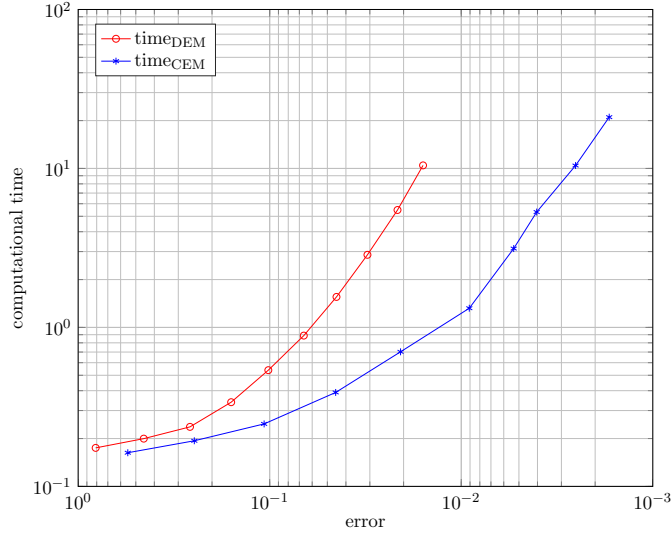


Figure 3: error vs work plot for DEM and CEM.

we choose the following form for  $V$

$$V = 0.1 \begin{cases} -2x - 1, & x < -0.5, \\ 4x + 2, & -0.5 \leq x < 0, \\ -2x + 2, & 0 \leq x < 0.5, \\ 4x - 1, & x \geq 0.5. \end{cases} \quad (30)$$

This is a linear interpolation of the function  $V$  we used in the smooth case above in the points  $\{-1, -0.5, 0, 0.5, 1\}$  (Figure 4). This case is of particular interest, since if the function  $f$  is the result of a numerical method on a  $PDE$ , it could not be smooth as in the previous case. We perform DEM and CEM with the same parameters as before, *i.e.*,  $M = 10000, N = 2^i, i = 3, \dots, 12$ . In Figure 5 it is possible to remark that the rate of convergence of DEM is unvaried with respect to the previous case. The CEM method experiences a slight decrease in the order of convergence with respect to the smooth case.

### 1.3.3 Numerical approximation of $\Phi$ with the PDE approach

Let us consider  $D$  as the interval  $[l, r]$ , the boundary condition in  $l$  to be fixed to killing and in  $r$  to be either killing or reflecting. In this case and for  $f, g$  independent of  $t$ , (22) can be written as the following initial value PDE

$$\begin{cases} -\frac{\partial}{\partial t}\Phi + f\frac{\partial}{\partial x}\Phi + \frac{1}{2}g^2\frac{\partial^2}{\partial x^2}\Phi = 0, & l < x < r \\ \Phi(l) = 1, \\ \Phi(r) = 1, & \text{if for } x = r \text{ the boundary is } \textit{killing} \\ \frac{\partial}{\partial x}\Phi(r) = 0, & \text{if for } x = r \text{ the boundary is } \textit{reflecting} \end{cases} \quad (31)$$

This equation can be solved, *e.g.*, using finite differences. If the implicit Euler scheme is employed for integration on a equispaced grid in space defined by the interval  $\Delta_x$  and in time by the step size  $\Delta_t$ , denoting by  $\Phi_j^k$  the solution at the  $j$ -th node and the  $k$ -th



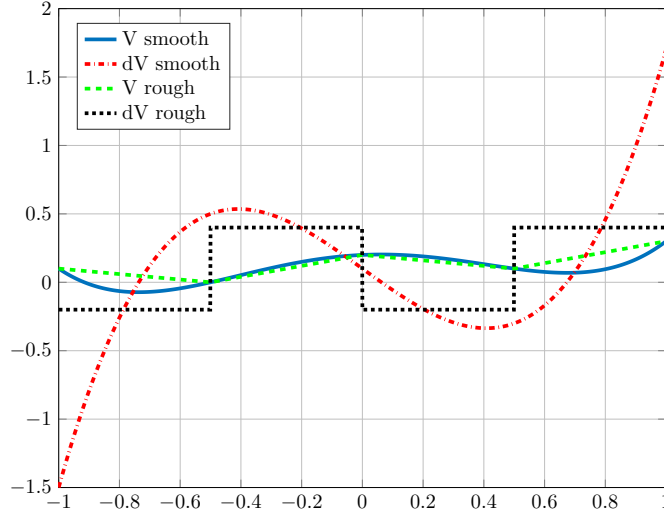


Figure 4:  $V$  and  $dV$  employed in the numerical experiments in both the smooth and rough cases.

time point and by  $f_j = f(j\Delta_x)$ ,  $g_j = g(j\Delta_x)$ , the solution is found solving iteratively the following linear system

$$-\frac{1}{2}\left(-f_j\frac{\Delta_t}{\Delta_x} + g_j^2\frac{\Delta_t}{\Delta_x^2}\right)\Phi_{j-1}^{k+1} + \left(1 + g_j^2\frac{\Delta_t}{\Delta_x^2}\right)\Phi_j^{k+1} - \frac{1}{2}\left(f_j\frac{\Delta_t}{\Delta_x} + g_j^2\frac{\Delta_t}{\Delta_x^2}\right)\Phi_{j+1}^{k+1} = \Phi_j^k. \quad (32)$$

The solution of this equation does not imply an high computational time, therefore one can choose  $\Delta_x$  and  $\Delta_t$  to be small. Proceeding in this way, the value of  $\Phi$  obtained with finite differences could be used as a reference value for estimating the error of DEM and CEM.

#### 1.3.4 Numerical experiments - Estimation of $\Phi$

**Smooth case.** We consider (23) with  $D = [-1, 1]$ , the final time  $T = 1$  and we define

$$\begin{aligned} f(x) &= -V'(x), \text{ where } V(x) = 8x^4 - 8x^2 + x + 2, \\ g(x) &= \sigma = 1.5. \end{aligned} \quad (33)$$

As in the approximation of  $\tau$ , we perform a Montecarlo simulation over  $M = 10000$  trajectories. We consider  $N = 2^i, i = 5, 6, \dots, 12$  and we compare the value of the exit probability given by DEM and CEM, comparing it with the value of the solution given by Finite Differences for  $X_0 = 0$ .

#### 1.4 Two-dimensional case

We are interested in estimating the exit time of a particle from a domain  $D \subset \mathbb{R}^2$ . Given  $W(t)$  a vector of two independent Brownian motions, we consider the equation (1). In this case,  $f: \mathbb{R}^2 \rightarrow \mathbb{R}^2, g: \mathbb{R}^2 \rightarrow \mathbb{R}^{2 \times 2}$ . We compute the mean exit time and the exit probability using DEM and CEM and compare results with the numerical solution of the PDE's presented in 1.2.

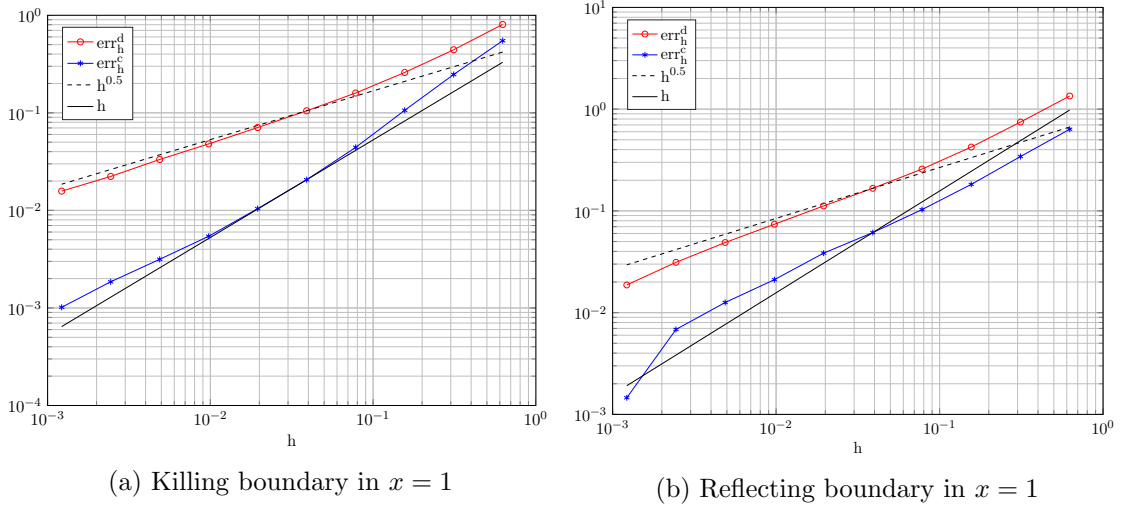


Figure 5: Orders of convergence for DEM and CEM in the one-dimensional case with  $f$  piecewise constant.

#### 1.4.1 Numerical experiments - Estimation of $\tau$

**Killing boundary conditions.** We consider a simple case of (1) in  $D = [-1, 1] \times [-1, 1]$ , where

$$f = 0 \in R^2, \quad g = \sigma I \in R^{2 \times 2}, \quad \sigma \in \mathbb{R}.$$

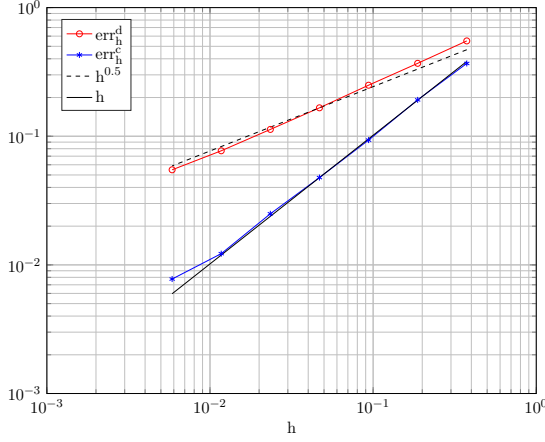
Moreover, we consider  $\partial D$  to be a killing boundary. The solution in this case is a Brownian motion. In this case, the partial differential equation (20) reduces to

$$\begin{cases} -\sigma^2 \Delta \bar{\tau} = 2, & \text{in } D, \\ \bar{\tau} = 0, & \text{on } \partial D. \end{cases} \quad (34)$$

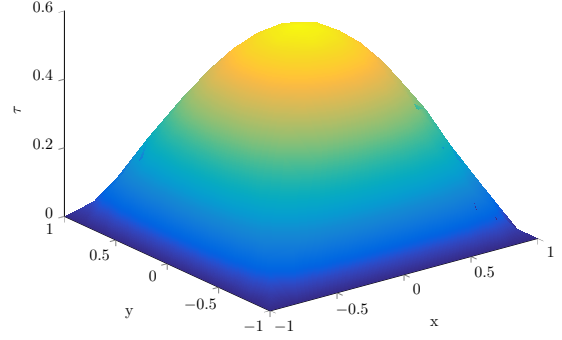
This is the Poisson equation, hence it is possible to solve it numerically with the Finite Elements Method or the finite differences avoiding a high computational cost. We use the Finite Elements Method adopting a regular mesh with equal constant spacing in the  $x$  and  $y$  directions, obtaining a solution as in Figure 6b. In order to verify the orders of convergence of DEM and CEM, we set  $T = 3$ ,  $\sigma = 1$ ,  $X_0 = (0, 0)^T$ , with  $M = 10000$  and  $N = 2^i, i = 3, \dots, 9$ . We then compare the Montecarlo estimation we obtain with the value of  $\bar{\tau}$  in  $(0, 0)$ , obtained by interpolation on the Finite Elements solution. The orders of convergence for this numerical experiment are shown in Figure 6a. The results confirm the theoretical orders of convergence for DEM and CEM, with an average order of 0.55 for DEM and 0.93 for CEM, which corrects to 0.98 if the last point is not taken into account.

**Mixed boundary conditions.** We consider the same problem as above with mixed killing and reflecting boundary conditions.  $f$  and  $g$  are the same as above, so the SDE model does not change, but we consider the two left and right boundaries of  $D$ , defined by  $x = \pm 1$ , to be reflecting. We denote this portion of the boundary as  $\Gamma_r$ , and the rest as  $\Gamma_k$ . In this case, the equation for  $\bar{\tau}$  becomes

$$\begin{cases} -\sigma^2 \Delta \bar{\tau} = 2, & \text{in } D, \\ \bar{\tau} = 0, & \text{on } \Gamma_k, \\ \partial \bar{\tau} \cdot n = 0, & \text{on } \Gamma_r. \end{cases} \quad (35)$$

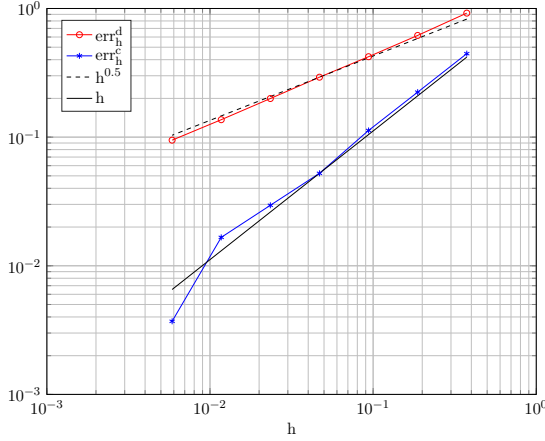


(a) Convergence of CEM and DEM.

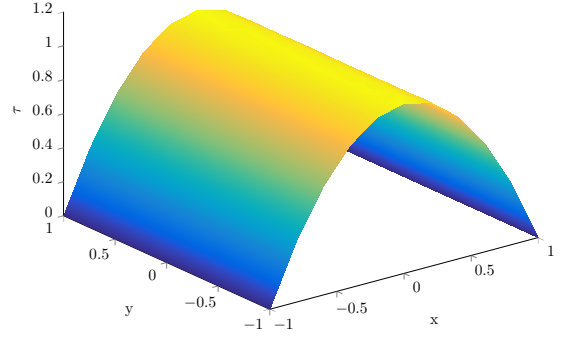


(b) Expectation of exit time.

Figure 6: Summary of the results for  $\tau$  in the two-dimensional case with pure killing boundary conditions.



(a) Convergence of CEM and DEM.



(b) Expectation of exit time.

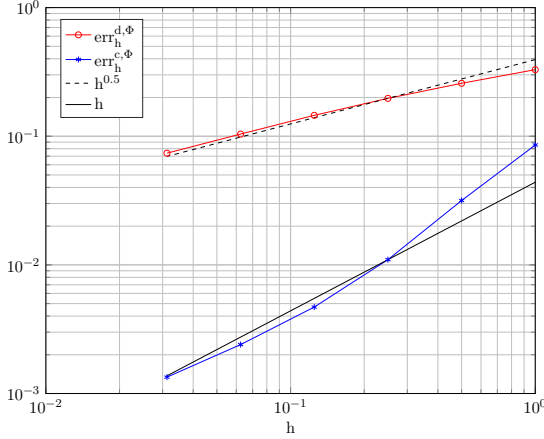
Figure 7: Summary of the results for  $\tau$  in the two-dimensional case with mixed boundary conditions.

The solution of this equation is shown in Figure 7b. We compute the expectation of  $\tau$  with DEM and CEM with the same parameters as above. The results (Figure 7a), show that the theoretical orders of convergence are not spoiled by this choice of boundary conditions. The mean order for DEM in this case is 0.55, while for CEM it is 1.15.

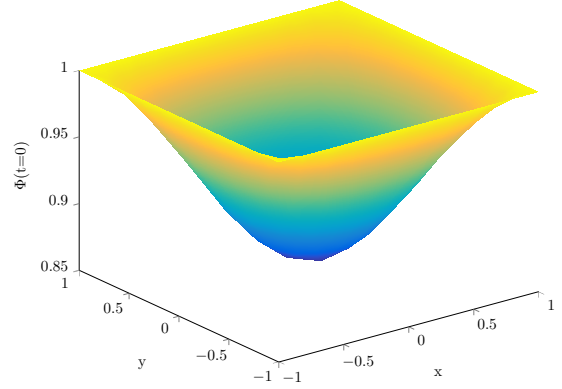
#### 1.4.2 Numerical experiments - Estimation of $\Phi$

**Killing boundary conditions.** We consider the same simple case as in section 1.4.1. We consider  $\partial D$  to be a killing boundary. The solution of (1) is in this case a Brownian motion. In this case, the partial differential equation (22) reduces to

$$\begin{cases} \frac{\partial}{\partial t} \Phi(x, t, T) + \frac{1}{2} \sigma^2 \Delta \Phi(x, t, T) = 0, & \text{in } D, 0 \leq t < T, \\ \Phi(x, t, T) = 1, & \text{on } \partial D, 0 \leq t < T, \\ \Phi(x, T, T) = 0, & \text{in } D. \end{cases} \quad (36)$$



(a) Convergence of CEM and DEM.



(b) Probability of exit.

Figure 8: Summary of the results for  $\Phi$  in the two-dimensional case with pure killing boundary conditions.

We solve this problem numerically with the Finite Elements Method as for (34). The solution at  $t = 0$  is shown in Figure 8b. We verify the orders of convergence of DEM and CEM setting  $X_0 = (0, 0)^T, \sigma = 1, T = 1$ . We consider  $M = 100000$  trajectories and  $N = 2^i, i = 0, \dots, 5$ . We then compare the Montecarlo estimation with the value of  $\Phi$  in  $(0, 0)$ , obtained by interpolation on the Finite Elements solution. The orders of convergence for this numerical experiment are shown in Figure 8a. The theoretical orders of convergence are confirmed in this case as well, with an average order of 0.43 for DEM and 1.19 for CEM.

**Mixed boundary conditions.** We consider the same values for the parameters, the time integration and the Montecarlo estimation as in the pure killing case. In this case, we set the boundary conditions to be reflecting on the subset of the boundary of  $D$  defined by  $x = \pm 1$  and killing for the other boundaries. Therefore, in this case the exit probability  $\Phi$  is the solution of the following PDE

$$\left\{ \begin{array}{l} \frac{\partial}{\partial t} \Phi(x, t, T) + \frac{1}{2} \sigma^2 \Delta \Phi(x, t, T) = 0, \quad \text{in } D, 0 \leq t < T, \\ \Phi(x, t, T) = 1, \quad \text{on } \Gamma_k, 0 \leq t < T, \\ \nabla \Phi(x, t, T) \cdot n = 0, \quad \text{on } \Gamma_r, 0 \leq t < T, \\ \Phi(x, T, T) = 0, \quad \text{in } D. \end{array} \right. \quad (37)$$

The solution of this equation computed with Finite Elements is shown in Figure 9b. The convergence results for DEM and CEM are shown in Figure 9a. The mean orders in this case are 0.37 for DEM and 0.87 for CEM, which is less than the prediction given by theoretical results. This decrease in the convergence rate is remarkable for small values of  $h$ . This could mean that the error caused by the Finite Element approximation of the solution of (36) is not negligible with respect to the error of CEM.

## 2 The uncertain Darcy problem

The two methods for approximating the mean exit time have been investigated in a general frame. In the following we will consider (1) with  $f: \mathbb{R}^2 \rightarrow \mathbb{R}^2$  given by the solution of the uncertain Darcy problem.

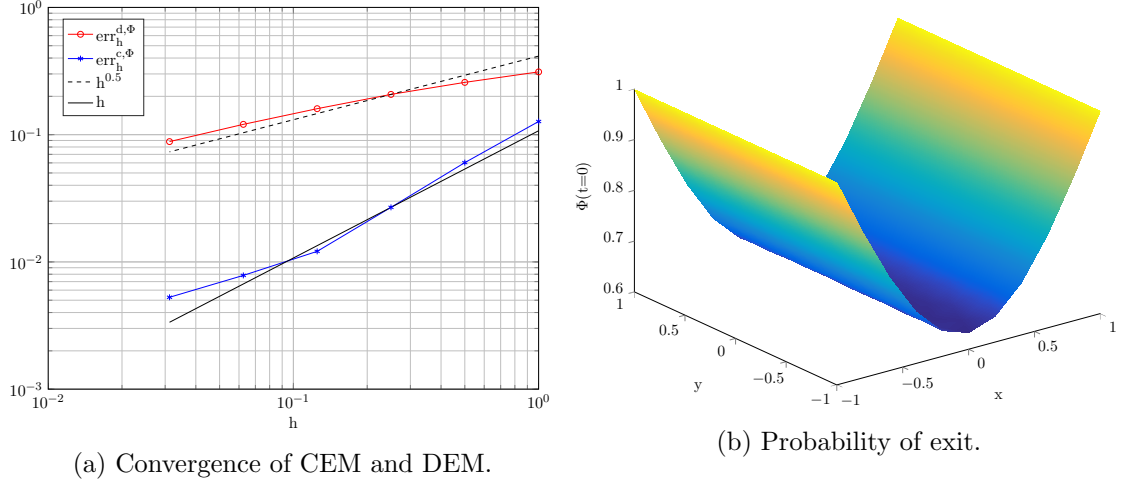


Figure 9: Summary of the results for  $\Phi$  in the two-dimensional case with mixed boundary conditions.

## 2.1 Problem statement

Let us consider a domain  $D \subset \mathbb{R}^2$ . Let us define the Neumann boundaries of  $D$  as  $\Gamma_N$ , its inlet boundary as  $\Gamma_{in}$  and its outlet boundary as  $\Gamma_{out}$ . Then, we search the solution of the following problem

$$\begin{cases} u = -A\nabla p, & \text{in } D, \\ \nabla \cdot u = 0, & \text{in } D, \\ p = p_0, & \text{on } \Gamma_{in}, \\ p = 0, & \text{on } \Gamma_{out}, \\ \nabla p = 0, & \text{on } \Gamma_N, \end{cases} \quad (38)$$

where  $A$  is a random field. The solution  $u$  of this equation is used as transport field in equation (1), which can be therefore written as

$$\begin{cases} dX(t) = u(X)dt + \sigma dW(t), & 0 < t \leq T, \\ X(0) = X_0, & X_0 \in D, \end{cases} \quad (39)$$

where we set the boundary conditions to be reflecting on  $\Gamma_N$  and killing on both  $\Gamma_{in}, \Gamma_{out}$ .

## 2.2 Finite Elements solution of the Darcy problem

Let us consider the domain  $D = [-1, 1] \times [-1, 1]$ . The random field  $A$  in (37) is chosen to be lognormal, *i.e.*,

$$A = e^\gamma, \quad (40)$$

where  $\gamma$  is a normal random field defined by its covariance function  $\text{cov}_\gamma(x_1, x_2)$  for any couple of points  $x_1, x_2$  in the domain  $D$ . The covariance function is of the Matern family, thus having the following form

$$\text{cov}_\gamma(x_1, x_2) = \frac{\sigma^2}{\Gamma(\nu)2^{\nu-1}} \left( \sqrt{2\nu} \frac{|x_1 - x_2|}{L_c} \right)^\nu K_\nu \left( \sqrt{2\nu} \frac{|x_1 - x_2|}{L_c} \right), \quad \nu \geq 0.5, \quad (41)$$

where  $\sigma^2$  is the variance,  $L_c$  is the correlation length,  $\Gamma$  is the gamma function,  $K_\nu$  is the modified Bessel function of the second kind and  $\nu$  is a parameter. Let us remark that

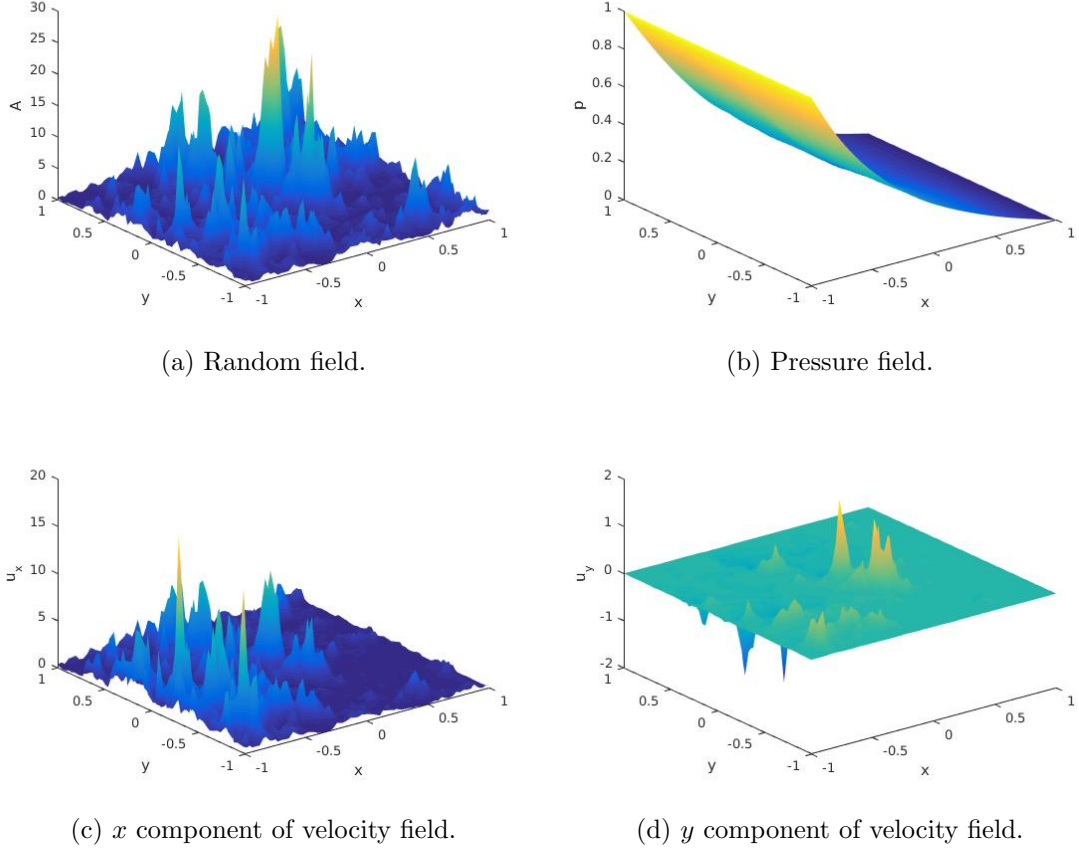


Figure 10: Approximate solution of the uncertain Darcy problem.

the covariance function does not depend on  $x_1, x_2$  but only on their euclidean distance  $|x_1 - x_2|$ . The regularity of the covariance function and of the realizations of  $A$  depend on  $\nu$ . In particular, for  $\nu$  equal to 0.5, the covariance is Lipschitz continuous and the field is  $\alpha$ -Hölder continuous for  $\alpha < 0.5$ . Results concerning regularity properties of  $A$  can be found in [7]. The realizations of  $A$  are computed using a discrete Fourier transformation on the vertices of a grid of  $D$ , equispaced on both the  $x$  and  $y$  directions with the same spacing  $\Delta_A$ . Then, the numerical solution  $p_h$  of (37) is obtained with linear Finite Elements on a regular mesh  $T_p$  with maximum element size  $\Delta_p$ . Since the vertices of the grid on which we compute  $A$  do not coincide with the vertices of  $T_p$ , we interpolate  $A$  on  $T_p$  to obtain  $p_h$ . Then, the velocity field  $u_h$  is retrieved computing the gradient on  $p_h$ . The results for a realization of  $A$  are shown in Figure 10, where the value of the inlet pressure  $p_0$  is equal to 1, and the parameters for the random field are  $\nu = 0.5, L_c = 0.05$ .

### 2.3 Solution of the SDE

Once the Finite Element approximation  $u_h$  of the velocity field is available, it is possible to approximate by means of DEM and CEM the solution of (38). The values of the numerical solution  $X_h$  can take any value in  $D$ , therefore it is necessary that the velocity field is defined in any point in  $D$ . If an interpolation of  $u_h$  is performed at each step, both DEM and CEM lose in computational efficiency. Hence, an interpolation of  $u_h$  has

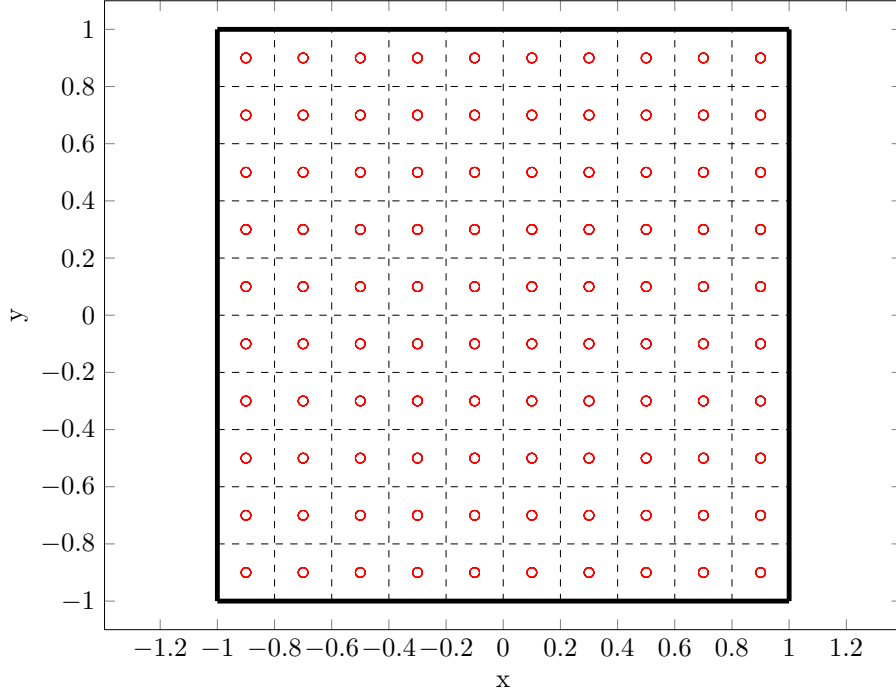


Figure 11: Grid used for interpolation of  $u_h$ . The interpolation points are represented in red.

to be performed before the numerical integration of the SDE. We choose to exploit the grid defined by  $\Delta_A$ , interpolating the values of  $u_h$  in the center of each square (Figure 11). Let us denote by  $Q$  the set of the interpolation points, whose elements are defined by

$$\{Q\}_{ij} = (-1 + (i - 0.5)\Delta_A, \quad -1 + (j - 0.5)\Delta_A)^T, \quad i, j = 1, \dots, \frac{2}{\Delta_A} =: N_A. \quad (42)$$

We compute two matrices  $U_x, U_y$  of  $\mathbb{R}^{N_A \times N_A}$  containing the values of the two components of  $u_h$  interpolated on the points of  $Q$ . Then, the velocity field is considered to be piecewise constant in each square of the grid defined by  $\Delta_A$ . Therefore, if we denote by  $\tilde{u}$  the transport field for the SDE, at the  $i$ -th step of the integration  $\tilde{u}$  is evaluated as follows

$$\tilde{u}(X_h(t_i)) = \begin{pmatrix} U_x(\lceil (X_{h,1}(t_i) + 1)/\Delta_A \rceil, \lceil (X_{h,2}(t_i) + 1)/\Delta_A \rceil) \\ U_y(\lceil (X_{h,1}(t_i) + 1)/\Delta_A \rceil, \lceil (X_{h,2}(t_i) + 1)/\Delta_A \rceil) \end{pmatrix}, \quad (43)$$

where  $X_{h,1}, X_{h,2}$  denote the first and second components of  $X_h$  and  $U_x(i, j)$  represents the element  $(i, j)$  of the matrix  $U_x$  (respectively  $U_y$ ). Then, given the step size  $h$ , one step of DEM will be defined as

$$X_h(t_{i+1}) = \tilde{u}(X_h(t_i))h + \sigma(W(t_{i+1}) - W(t_i)). \quad (44)$$

Given an input initial value  $X_0$  for (38), we approximate the solution using DEM and CEM using the strategy above. In Figure 12 we display 15 trajectories for  $X_0 = (-0.8, -0.8)^T$  with two different timesteps. The choice of the initial point is made in order to observe reflections on the lower boundary of the domain  $D$  on which we compute the solution, as well as the killing boundary at the left side.

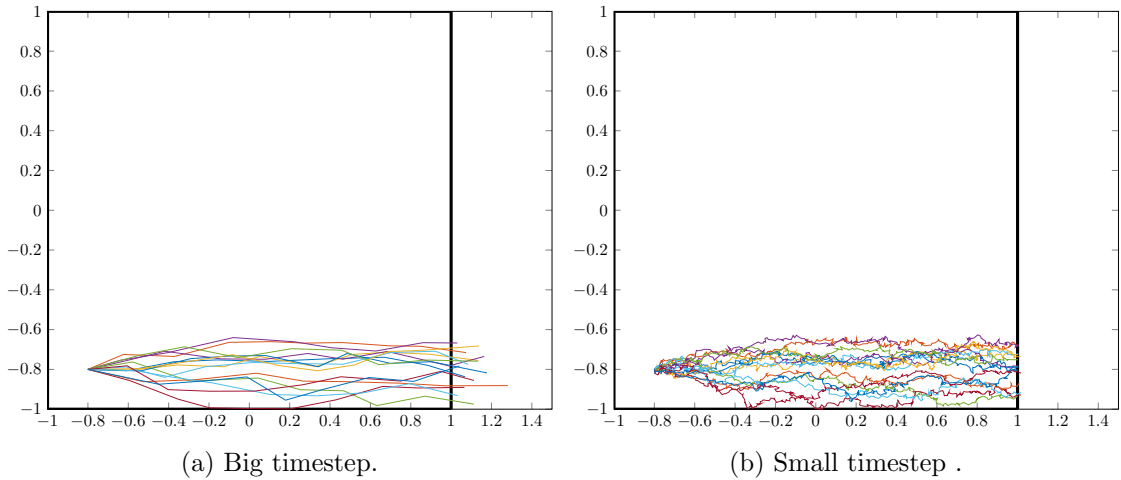


Figure 12: Trajectories of the numerical solution of (38) with DEM.

## References

- [1] E. GOBET, *Weak approximation of killed diffusion using Euler schemes*, Stochastic Processes and their Applications, 87 (2000), pp. 167–197.
- [2] E. GOBET, *Euler schemes and half-space approximation for the simulation of diffusion in a domain*, ESAIM: Probability and Statistics, 5 (2001), pp. 261–297.
- [3] E. GOBET AND S. MENOZZI, *Stopped diffusion processes: boundary correction and overshoot*, Stochastic Processes and their Applications, 120 (2010), pp. 130–162.
- [4] D. S. GREBENKOV AND R. VOITURIEZ, *Exit time distribution in spherically symmetric two-dimensional domains*, (2014), pp. 1–34.
- [5] D. J. HIGHAM, X. MAO, M. ROJ, Q. SONG, AND G. YIN, *Mean Exit Times and the Multilevel Monte Carlo Method*, SIAM/ASA Journal on Uncertainty Quantification, 1 (2013), pp. 2–18.
- [6] S. KRUMSCHEID, M. PRADAS, G. A. PAVLIOTIS, AND S. KALLIADASIS, *Data-driven coarse graining in action: Modeling and prediction of complex systems*, Physical Review E, 92 (2015), p. 042139.
- [7] F. NOBILE AND F. TESEI, *A Multi Level Monte Carlo method with control variate for elliptic PDEs with log-normal coefficients*, Stochastic Partial Differential Equations: Analysis and Computations, (2015), pp. 1–47.
- [8] G. A. PAVLIOTIS, *Stochastic Processes and Applications*, 2014.
- [9] L. SIROVICH, J. E. MARSDEN, AND S. S. ANTMAN, *Theory and Applications of Stochastic Processes: An Analytical Approach*, vol. 170, Springer, 2010.